ARTICLE
Traditional Medicine Research 2022;7(6):53. https://doi.org/10.53388/TMR20220419004

Oriental Medicine

Platycladus orientalis shells promote melanogenesis via p38, AKT and Wnt/β-catenin signaling pathways

Fu-Rui Liu[1], Hao Xiang[1], Qian-Bei Guo[1], Shu-Li Man[1*], Long Ma[1*]

[1]State Key Laboratory of Food Nutrition and Safety, Key Laboratory of Industrial Microbiology, Ministry of Education, Tianjin Key Laboratory of Industry Microbiology, National and Local United Engineering Lab of Metabolic Control Fermentation Technology, China International Science and Technology Cooperation Base of Food Nutrition/Safety and Medicinal Chemistry, College of Biotechnology, Tianjin University of Science & Technology, Tianjin 300457, China.

[*]**Corresponding to:** Shu-Li Man, College of Biotechnology, Tianjin University of Science & Technology, No. 29, 13th Street, Economic and Technological Development District, Tianjin 300457, China. E-mail: msl@tust.edu.cn. Long Ma, College of Biotechnology, Tianjin University of Science & Technology, No. 29, 13th Street, Economic and Technological Development District, Tianjin 300457, China. E-mail: malong@tust.edu.cn.

Author contributions

Fu-Rui Liu analyzed data, investigated, wrote and edited the manuscript. Hao Xiang and Qian-Bei Guo performed original draft writing, formal analysis and visualization of data. Shu-Li Man and Long Ma reviewed and edited the manuscript, performed conceptualization, methodology and funding acquisition.

Competing interests

The authors declare no conflicts of interest.

Acknowledgments

This work was supported by National Natural Science Foundation of China (No. 82074069, No. 32072309). We thank Prof. Long Ma for editing the English text of a draft of this manuscript.

Abbreviations

POS, *Platycladus orientalis* shells; GC-MS, gas chromatography – mass spectrometry; TYR, tyrosinase; MTT, microwave thermoacoustic tomography; GSK-3β, glycogen synthase kinase-3β; JNK, c-Jun N-terminal kinase; MAPK, mitogen-activated protein kinase; ERK, extracellular signal-regulated kinases; MITF, microphthalmia-associated transcription factor; RT, room temperature; SEM, standard error mean; TRP, tyrosinase-related protein.

Peer review information

Traditional Medicine Research thanks all anonymous reviewers for their contribution to the peer review of this paper.

Citation

Liu FR, Xiang H, Guo QB, Man SL, Ma L. *Platycladus orientalis* shells promote melanogenesis via p38, AKT and Wnt/β-catenin signaling pathways. *Tradit Med Res*. 2022;7(6):53. doi: 10.53388/TMR20220419004.

Executive editor: Guang-Ze Ma.

Received: 19 April 2022; **Accepted:** 14 May 2022; **Available online:** 03 June 2022.

Abstract

Background: *Platycladus orientalis*, which has been employed in traditional Chinese medicine for cool blood, antibacterial, promotion of hair growth and therapy of poliosis for centuries. However, there have been few reports focusing on *Platycladus orientalis* shells treating pigmentary disorders. **Methods:** In present study, gas chromatography – mass spectrometry was applied to analyzing the volatile composition of *Platycladus orientalis* shells and cellular metabolism. Experiments in vivo were carried out to evaluate the effect of *Platycladus orientalis* shells treating pigmentation disorders in C57BL/6J mice. **Results:** Our results indicated that cedrol occupied the largest percentage in *Platycladus orientalis* shells (17.1%). Meanwhile, *Platycladus orientalis* shells up-regulated the content of palmitic acid and increased melanin content and tyrosinase activity. Its mechanism possibly involved in the inhibiting phosphorylation of AKT and β-catenin, increasing phosphorylation of p38 to promote microphthalmia-associated transcription factor expression. The animal experiment also proved that *Platycladus orientalis* shells promoted melanogensis and hair blacken in C57BL/6J mice. **Conclusion:** All in all, *Platycladus orientalis* shells potentially promoted melanogenesis in vitro and in vivo. Cedrol was regarded as the main active substance in *Platycladus orientalis* shells. Therefore, it could be used for treatment of pigmentary disorders under safe concentration in the prospective application.

Keywords: GC-MS; *Platycladus orientalis* shells; melanogenesis; tyrosinase; pigmentary disorders

Highlights

In this paper, cedrol was obtained as the main active substances in *Platycladus orientalis* shells by gas chromatography – mass spectrometry analysis. Then we found that *Platycladus orientalis* shells could promote melanogensis and improve tyrosinase activity through in vivo and in vitro experiments. The mechanism may involve inhibition of AKT and β-catenin phosphorylation, increasing the phosphorylation of p38 to promote the expression of microphthalmia associated transcription factors.

Medical history of objective

Platycladus orientalis as an ancient traditional Chinese medicine displays a medical value due to its anti-inflammatory, antioxidant, immuno-modulatory, anti-hepatitis B virus, promoting hair growth and other activity. According to the records of *Chinese Tibetan Materia Medica* (compiled in 1997 by Da-Shang Luo), its leaves can be used to treat hematemesis, hair loss caused by blood heat and premature gray hairs. Besides, *Platycladus orientalis* shells are universally used in haemostatic, expectorant and anti-cough remedies.

Background

Platycladus orientalis as an ancient traditional Chinese medicine displays a huge medical value due to its anti-inflammatory, antioxidant, immuno-modulatory, anti-hepatitis B virus, promoting hair growth and other activity [1–4]. According to the records of *Chinese Tibetan Materia Medica* (compiled in 1997 by Da-Shang Luo), its leaves can be used to treat hematemesis, hair loss caused by blood heat and premature gray hairs. Besides, *Platycladus orientalis* shells (POS) are universally used in haemostatic, expectorant and anti-cough remedies [5]. In previous reports, its leaves promoted hair regrowth by inducing hair follicles to enter anagen from dormancy phase and inhibiting the 5α-reductase activity [6, 7]. However, there have been few reports focus on the POS treating pigmentary disorders. Cedrol as the main active ingredient of *Platycladus orientalis* had the potential of becoming a new hair growth promoter [8]. It also prevented hair follicle dystrophy and provided local protection against chemotherapy-induced alopecia [9].

Melanin produced by melanocytes was distributed in hair, eye and skin [10]. It possessed many physiological functions including protection against the skin damage and scavenging reactive oxygen species [11]. However, the abnormal accumulation of melanin caused dermatological problems such as freckles, melasma and poliosis, as well as vitiligo [12]. Hair graying was another inevitable process of aging [13]. The regulation of melanogenesis was important for treating these diseases [14]. Tyrosinase (TYR), as an important rate-limiting enzyme of melanogenesis, which involved in the catalysis of tyrosine and its metabolite (DOPA), ultimately generated melanin in melanosomes [15, 16]. Microphthalmia-associated transcription factor (MITF) was a main regulator in the expression of related enzymes [17]. Therefore, TYR and MITF were two of the important regulative points for melanogenesis in melanocytes.

Up to now, the pharmacological effect of POS regulated melanogenesis was remain unclear. Our research firstly reported the phenomenon and possible mechanisms of POS promoting melanogenesis from the cellular level and C57BL/6J mouse model of H_2O_2-induced hair fading.

Methods

Plant material

POS and cedrol were collected in September 2017 from Qiyun biological technology Co., Ltd., Guangzhou, China. They was identified by Prof. Man. A voucher specimen (MSPOS201709) was deposited in Tianjin University of Science & Technology, Tianjin, China.

Preparation of the plant extract

The air-dried POS (10 g) was extracted with 150 mL of methanol and ethyl acetate in a soxhlet apparatus during 3 h, respectively. Then the samples were evaporated using a rotary evaporator. The residuum was rinsed with 10 mL of 75% ethonal solvent. The extract was storage at 4 ˚C preparing for further research. The methanol extract which showed better effect on TYR in potatoes than ethyl acetate extract did. Therefore, the methanol extract of POS was utilized for further research. Voucher specimens (MSPOS201801) were deposited at College of Biotechnology in Tianjin University of Science & Technology.

Gas chromatography – mass spectrometry (GC-MS) analysis of POS

GC-MS analysis was performed with an Agilent 7890A gas chromatography (Agilent Technologies Co., Ltd., Santa Clara, CA, USA) coupled to an Agilent 5975C mass selective detector (Agilent Technologies Co., Ltd.) and Agilent ChemStation software (Agilent Technologies Co., Ltd.). The inlet temperature was set at 260 ˚C and an injection of 1 μL was made with split ratio of 20:1. Helium was used as carrier gas at a flow rate of 1.0 mL/min. The analysis was carried out in the splitless mode. A 5 min solvent delay was used to avoid acquiring unnecessary data. Programmed temperature was applied to obtain the separation of the analysis. Precisely the initial temperature was 70 ˚C then ramped at 5 ˚C/min to 300 ˚C. The gas chromatograph was interfaced with a micro-channelplates plus mass detector operating in the electron impact ionization mode (70 eV) under auto-tune conditions. The temperatures of ionization source and transfer line were 220 ˚C and 250 ˚C, respectively. The data output was achieved using scanning mode for identification and selected ion monitoring mode for quantification.

Assay of TYR activity in potatoes

The TYR activity of POS in potatoes were measured according to the method previously described [15]. Twenty grams of the frozen potato root were homogenized in a liquefier with 40 mL of 0.1 M phosphate buffer (pH 6.8) for 2 min at 4˚C. The suspension was filtered through four layers of cheesecloth and centrifuged at 4,000 rpm for 10 min at 4 ˚C. Then the supernatant was stored at this temperature in a refrigerator and utilized as the TYR solution. The reaction system (0.2 mL) for TYR activity assay containing L-DOPA solution (50 μL, 10 mM) was mixed with phosphate buffer (70 μL, 0.1 M, pH = 6.8) and incubated at 25 ˚C for 10 min. Subsequently, 1 μL of different concentrations of POS and 80 μL of the TYR solution were continuously added to the above solution. The action of TYR was determined spectrophotometrically at 492 nm (measurement of o-dopaquinone product). All determinations were performed in triplicate.

Cell culture

Mouse B16F10 melanoma cells were obtained from the Cell Resource Center, Peking Union Medical College (Beijing, China). The cells were maintained in Dulbecco's modified Eagle medium with 10% heat-inactivated fetal bovine serum, 100 U/mL penicillin and 100 μg/mL streptomycin at 37 ˚C (5% CO_2).

Microwave thermoacoustic tomography (MTT) assay

Cell viability was determined by a colorimetric assay using MTT. Cells were seeded at a density of 1×10^4/well in a complete growth medium in 96-well plates. The cells were incubated with the test compounds for 24 h before the MTT assay. Then, a fresh solution of MTT (0.5 mg/mL) was added to each single well with a further incubation for 4 h. Finally, the cell substrates were dissolved with 100 μL of dimethyl sulfoxide and then optical densities were analyzed in a multiwall plate reader at 570 nm (BioTek Instruments, Inc., Winooski, VT, USA). All determinations were performed in triplicate.

Measurement of cellular melanin content

The melanin content in cells were measured according to the method previously described [18]. 1×10^5 B16F10 cells were seeded in 6-well plates and cultured at 37 °C overnight. Then the cells were treated with various concentrations of POS (0, 1, 2 μg/mL) or cedrol (0, 0.1, 0.2 μg/mL). After incubation, each plate was washed with polybutylene succinate twice and lysed in 100 μL of 1 M NaOH. The lysate was heated at 80 °C for 30 min and then determined in a multiwall plate reader at 400 nm (BioTek Instruments, Inc., Winooski, VT, USA). All determinations were performed in triplicate.

Measurement of cellular TYR activity

The TYR activity of POS in potatoes was measured according to the method previously described [15]. 1×10^5 B16F10 cells were seeded in 6-well plates and cultured at 37 °C overnight. Then the cells were treated with various concentrations of POS or cedrol. After incubation, each plate was washed with PBS twice, lysed in 225 μL of 1% TritonX-100 and then stored at −80 °C for 1 h. After thawed twice and centrifuged for 10 min at 12,000 rpm, the supernatant (50 μL) was added in a 96-well plate and mixed with 100 μL of 0.5% L-DOPA for incubation at 37 °C for 1 h. Optical densities were measured in a multiwall plate reader at 490 nm (BioTek Instruments, Inc., Winooski, VT, USA). All determinations were performed in triplicate.

GC-MS analysis of metabolism in B16F10 cells

B16F10 cells were seeded at 37 °C and treated with 1 μg/mL of POS for 24 h. Collecting cells and the change of the metabolites in B16F10 cells was measured by GC-MS. The cells were treated with precooling methanol and thawed in ultrasound bath at 50 Hz for 15 min (Jining Hengtong Ultrasonic Electronic Equipment Co., Ltd., Jining, China). After centrifuged at 12,000 rpm for 10 min, the supernatant (500 μL) was collected and vacuum-dried. The dried extracts were dissolved in 50 μL of methoxyamine solution (15 mg/mL) in pyridine and shaken at 70 °C for 1 h to protect aldehyde and ketone groups. Then 50 μL of bis(trimethylsilyl)trifluoroacetamide was added for trimethylsilylation of acidic protons and shaken at 37 °C for 1 h. 150 μL of n-heptane (1 mg/mL of docosane) was added and centrifuge at 10,000 rpm for 5 min. Supernatant was immediately transferred to a clear glass autosampler vials (Thermo Fisher Scientific, Waltham, MA, USA) and analyzed by GC-MS.

Immunofluorescence analysis

B16F10 cells were fixed in 4% paraformaldehyde at 4 °C for 30 min. 0.02% polyethylene glycol sorbitan monolaurate (Tween-20) in PBS was used to permeabilize cells for 10 min after triple PBS wash. Cells were incubated with primary antibodies (1:1,000 dilute in PBS contain 3% bovine serum albumin) at room temperature (RT) for 2 h and then incubated with goat anti-rabbit IgG (H + L) Alexa Fluor 594 secondary antibody. Nucleus was dyed by 4',6-diamidino-2-phenylindole (Solarbio Science & Technology Co., Ltd., Beijing, China) for 10 min at RT. Images were taken using laser scanning confocal microscope (Olympus, Tokyo, Japan).

Reverse transcriptase polymerase chain reaction

Total RNA was isolated from B16F10 cells using Trizol (Sangon Biotech Co., Shanghai, China). Polymerase chain reaction products were electrophorized on 3.0% agarose gel in which gel red nucleic acid stain (Biotium, CA, USA) was added. The intensity of gene was quantified by Image J software. The primer sequence and reaction temperature were manifested in Table 1.

Western blot analysis

Cells were lysed in radio immunoprecipitation assay buffer with PMSF (Solarbio Science & Technology Co., Ltd., Beijing, China). Equal amounts of protein samples were subjected to sodium dodecyl sulfate-polyacrylamide gel electropheresis (12%) and then transferred to poly(vinylidene fluoride) membrane (Merck Millipore Ltd., Billerica, MA, USA). poly(vinylidene fluoride) membrane was blocked in tris buffer solution with tween with 5% skim milk at RT for 1 h and incubated with primary antibodies for 8 h. The primary antibodies contained TYR, MITF, β-catenin (catenin beta-1), glycogen synthase kinase-3β (GSK-3β), phospho- GSK-3β (Ser 9), protein kinase Bα (AKT1/PKBα), phospho- AKT (Ser 473) (Bioworld Technology, St Louis, MN, USA), mitogen-activated protein kinase p38a/β (p38α/β) (A-12), c-Jun N-terminal kinase 1/mitogen-activated protein kinase 8 (JNK1/MAPK8), extracellular signal-regulated kinases 1/2 (ERK1/2) (BOSTER, Wuhan, China), phospho- SAPK/JNK (Thr183/Tyr185), phospho- p38 MAP kinase (Thr180/Tyr182) and phospho- p44/42 MAPK (ERK1/2) (Thr202/ Tyr204) (Cell Signalling Technology, Danvers, MA, USA). After triple tris buffer solution with tween wash, the membranes were incubated with second antibody for 3 h. Immunoblotting bands were detected by Odyssey infrared imaging system (LI- COR Biotechnology, Lincoln, NE, USA).

In vivo model of H_2O_2-induced hair fading

Twenty-four C57BL/6J mice (18–22 g, 4-week old) were purchased from Tianjin Yuda Laboratory Animal Breeding Co., Ltd. (License No. SCXK (Jin) 2021-0001, Tianjin, China). All the experiments were approved by national legislations of china and local guidelines (Tianjin University of Science & Technology 20200331). Briefly, it was carried out according to the method previously described [7]. The dorsal hairs of these mice were depilated (4 × 4 cm) by wax/resin mixture (1:3) and randomly divided into 3 groups (n = 8). (1) Normal group, after 30 min of 100 μL of normal saline treatment, 100 μL of 75% ethanol was applied topically to the shaved dorsum, once a day; (2) model group, after 30 min of 100 μL of hydrogen peroxide (5% hydrogen peroxide in water) treatment, 100 μL of 75% ethanol was applied topically to the shaved dorsum once a day; (3) POS group, after 30 min of 100 μL of 5% hydrogen peroxide treatment, 100 μL of POS (30 mg/mL of POS was dissolved in 75% ethanol) was applied topically to the shaved dorsum once a day.

Determination of melanin in mice hair

The mice dorsal hair was collected at the termination of the experiment. The equal weight of hair was put into the closed polytetrafluoroethylene container. The hair was hydrolyzed with 5 mL of 30% hydrochloric acid at 110–112 °C for 4 h. Then the hydrolysate was centrifugal at 12,000 rpm for 15 min. The precipitate was lysed in 100 μL of 1 M NaOH and then determined the absorbance by a multiwall plate reader at 400 nm (BioTek Instruments, Inc.).

Table 1 The primer sequence and annealing temperature

Gene	Nucleotide sequences for primers		Annealing temperature (°C)	Product (bp)
	Forward primer	Reverse primer		
TYR	ATCAGCTCAGTCTATGTCATCCC	CCAAGGCAGAAACCCTGGT	54.2	198
TRP-1	TCACCCTCAATTTGTCATTGCC	CGGGTCCTTCGTGAGAGAA	54.2	191
TRP-2	TTCCCCGAGTCTGCATGAC	TGCATGTCCGGTTGAAGAATTT	53.0	213
MITF	ACTTTCCCTTATCCCATCCACC	TGAGATCCAGAGTTGTCGTACA	49.2	143

TYR, tyrosinase; TRP, tyrosinase-related protein; MITF, microphthalmia-associated transcription factor.

Histopathological examination of skin

After six-week treatment, all of the mice were anesthesia with 5% chloral hydrate. A portion of the skin was cut and fixed in 10% formalin, followed by paraffin embedded. Five-micrometer-thick sections were prepared and stained with lillie staining. The melanin showed black. The hair follicle were observed and the melanin-containing hair follicle were counted under the light microscope (100×) (Olympus Optical Co., Ltd., Tokyo, Japan). Randomly chose three fields and calculated melanin production rate. Melanin production rate (%) = the number of melanin – containing hair follicle/total number of hair follicle) × 100%.

Statistical analysis

Statistical evaluation was conducted by using SPSS 17.0 for Windows package software. Data have been expressed as the means ± standard error mean (SEM). One-way variance analysis and Duncan multiple range test were used to determine significantly different groups. *P* values less than 0.05 were considered as significant differences for all statistical calculations.

Results

GC-MS analysis of POS

The chemical composition of POS methanol extract was analyzed by GC-MS. The results were shown in Table 2. The major components in the essential oil contained monoterpenes like 4-carene (4.7%), sesquiterpenes which were consisted of cedrol (17.1%), caryophyllene oxide (2.7%), caryophyllene (2.6%) and thujopsene (1.5%), esters such as 9, 17-octadecadienal (0.9%), 2-methyl-Z, Z-3, 13-octadecadienol (1.3%) and oleic acid (0.9%) and so forth. The chemical structures of some compounds in POS were shown in Figure 1A. Among them, cedrol is the most predominant component in the essential oil of POS.

POS and cedrol regulated TYR activity and melanin synthesis

In order to evaluate the influence of POS on melanogensis, TYR activity under POS exposure was measured in potatoes and melanocytes. As a result, POS displayed a concentration-dependent increase of potato TYR activity (Figure 2A). Moreover, it significant increased the activity of TYR (Figure 2B1) and the content of melanin (Figure 2B2) following incubation of POS at concentration of 1 and 2 μg/mL, respectively for 24 h, which showed no cytotoxicity in B16F10 cells (Figure 1B). Western blot (Figure 2C) and immunofluorescence analysis also indicated that POS significantly enhanced the expression of TYR in B16F10 cells (Figure 2D). Cedrol which was regarded as the mainly volatility component in POS promoted melanogenesis activity and markedly increased the activity of TYR (Figure 2E1) and the content of melanin (Figure 2E2) in B16F10 cells on 0.2 μg/mL.

POS regulated the metabolism of B16F10 melanocyte

Metabolomics analysis was carried out for explain the biochemistry mechanism of POS in the process of melanogensis, which was involved in eight metabolites including lactic acid, ethanedioic acid, glycerol, hexadecanoic acid, myo-Inositol, octadecanoic acid, fumaric acid and 1H-Indole-2-carboxylic acid. As a result, GC-MS data indicated that POS significantly increased the relative concentration of hexadecanoic acid, myo-Inositol, octadecanoic acid, fumaric acid and 1H-indole-2-carboxylic acid in B16F10 cells ($^{*}P < 0.05$) (Table 3).

Table 2 Chemical composition of essential oil from POS analyzed by GC-MS

Number	RT (min)	Compound[a]	Molecular formula	Peak area (%)
1	7.72	α-Pinene	$C_{10}H_{16}$	0.6
2	8.09	3-Carene	$C_{10}H_{16}$	0.9
3	8.89	β-Phellandrene	$C_{10}H_{16}$	0.1
4	9.80	β-Terpineol	$C_{10}H_{18}O$	0.6
5	13.04	Myrtenol	$C_{10}H_{16}O$	0.6
6	15.24	Bornyl acetate	$C_{12}H_{20}O_2$	1.0
7	16.89	4-Carene	$C_{10}H_{16}$	4.7
8	18.79	Caryophyllene	$C_{15}H_{24}$	2.6
9	19.08	Thujopsene	$C_{15}H_{24}$	1.5
10	19.63	α-Caryophyllene	$C_{15}H_{24}$	1.8
11	21.89	α-Farnesene	$C_{15}H_{24}$	0.2
12	22.83	Caryophyllene oxide	$C_{15}H_{25}O$	2.7
13	23.45	Cedrol	$C_{15}H_{26}O$	17.1
14	23.84	Seychellene	$C_{15}H_{24}$	0.5
15	35.11	Trans-13-Octadecenoic acid	$C_{18}H_{34}O_2$	0.3
16	36.52	(Z)-9,17-Octadecadienal	$C_{18}H_{32}O$	0.9
17	37.46	2-Methyl-Z,Z-3,13-octadecadienol	$C_{19}H_{36}O$	1.3
18	38.11	Oleic acid	$C_{18}H_{34}O_2$	0.9

[a]The components were identified by their mass spectra and retention indices with that of the Wiley and National Institute of Standards and Technology mass spectral databases and the previously published retention indices. POS, *Platycladus orientalis* shells; GC-MS, gas chromatography – mass spectrometry; RT, retention time.

Table 3 POS treatment impacted the content of metabolic markers in melanocytes (n = 4)

Number	RT (min)	Metabolites	POS to non-treated group
1	16.87	Ethanedioic acid	/-
2	20.76	Glycerol	/-
3	38.50	Hexadecanoic acid	↑*
4	39.69	Myo-inositol	↑*
5	41.93	Octadecanoic acid	↑*
6	44.35	Fumaric acid	↑*
7	53.07	1H-indole-2-carboxylic acid	↑*

$^{*}P < 0.05$, compared with non-treated group. ↑, indicated metabolites increase; /-, showed no significant changes; POS, *Platycladus orientalis* shells.

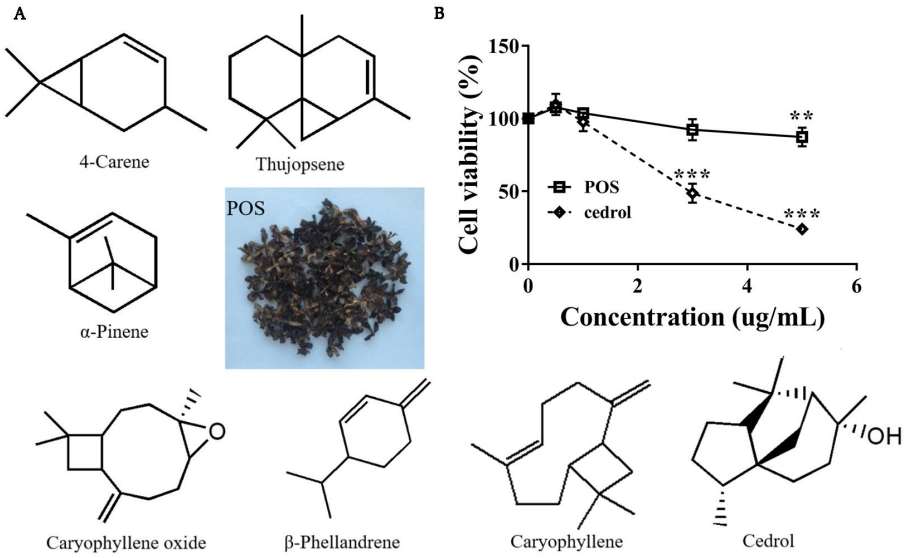

Figure 1 Structural formula and cytotoxicity of POS and cedrol. (A) Chemical structure of volatile oil identified from POS. (B) B16F10 cells survival curve via POS or cedrol treatment. Results represented the means ± SEM of three independent experiments. $^{**}P < 0.01$, $^{***}P < 0.001$, compared with non-treated group (0 μg/mL). SEM, standard error mean; POS, *Platycladus orientalis* shells.

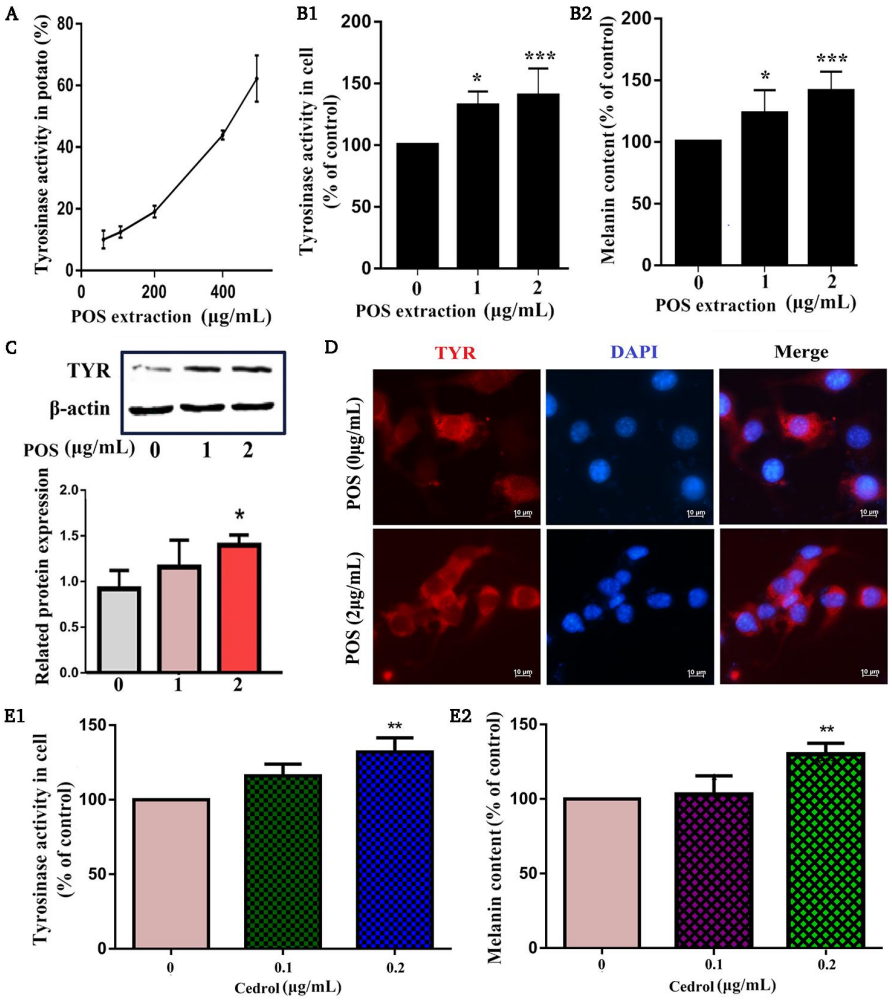

Figure 2 The regulation of melanogenesis in B16F10 cell. (A) Effect of POS on TYR activity in potatoes; (B1) effect of POS on TYR activity; (B2) melanin content in B16F10 cells; (C) western blot; (D) immunofluorescence analysis of TYR in B16F10 cells; (E1) effect of cedrol on TYR activity; (E2) melanin content in B16F10 cell. The TYR protein is shown in red, while the nucleus in blue. Data are representative of three independent experiments. $^{*}P < 0.05$, $^{**}P < 0.01$, $^{***}P < 0.001$, compared with non-treated group (0 μg/mL). POS, *Platycladus orientalis* shells; TYR, tyrosinase; DAPI, 4',6-diamidino-2-phenylindole.

POS mediated melanogenesis by regulating various signaling pathways

TYR and MITF were regarded as two important regulative proteins in melanogenesis. Reverse transcription – polymerase chain reaction analysis indicated that mRNA expression of TYR, TYR-related protein (TRP)-1, TRP-2 and MITF in B16F10 cells was concentration-dependently enhanced by POS treatment. Meanwhile, protein level of MITF was also increased. Subsequently, MITF associated signal pathways including MAPK, AKT and GSK-3β/β-catenin were investigated. As a result, POS significantly up-regulated the phosphorylation of GSK-3β and p38 and down-regulated protein level of GSK-3β and the phosphorylation of AKT compared with non-treated groups (Figure 3). Western blot results indicated that the protein expression of β-catenin was enhanced in POS treated cells. Immunostaining results showed a clear enrichment of β-catenin protein in the nuclear fraction of B16F10 cells upon POS treatment (Figure 4).

POS promoted melanogenesis and hair blacken in C57BL/6J mice

H_2O_2-induced obvious decolorization in mice hair. Photomicrographs of hair in all groups demonstrated that hair color in POS treated group more darker brown than that in model group. The melanin content in POS treated group was also higher than that in model group. The melanin production rate obtained from histological examination of skin sections indicated that POS enhanced the melanogenesis in mice dorsal skin (Figure 5).

Discussion

With the sharply increase of social pressure and environmental pollution, the incidence of canities and pigmentary disorders was surge ahead rapidly [19, 20]. Although there were numerous therapeutic regimens used for these diseases, few displayed efficient. In the previous research, *Platycladus orientalis* played a key role in the therapy of alopecia in many formulations [7]. However, there was no detailed report on the POS regulating melanin synthesis at present. According to the screening of different solvents, the methanol extract of POS containing volatile oil showed a better concentration-dependent increase of TYR activity in potatoes. It also increased melanin content and expression of TYR in melanocytes (Figure 2). Moreover, the vivo trial also verified that the methanol extract of POS could improve hair fade and skin dispigment in H_2O_2-induced C57BL/6J mice (Figure 5).

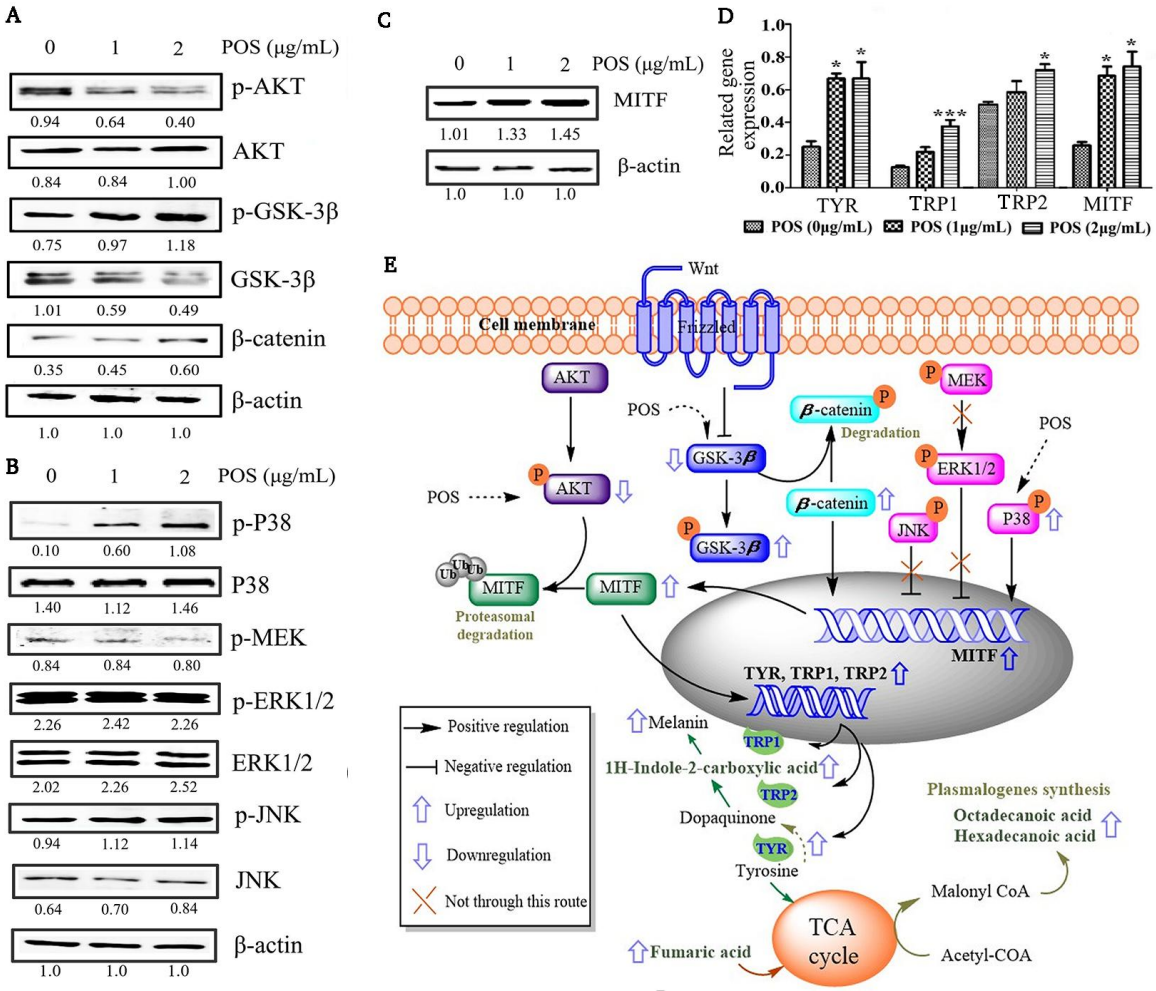

Figure 3 POS mediated melanogenesis by regulating various signaling pathways. (A) Western blot analysis of AKT and Wnt/β-catenin signaling pathway; (B) western blot analysis of MAPK signaling pathway; (C) the protein level of MITF in B16F10 cells; (D) effect of POS on mRNA of related genes (TYR, YRP1, TRP2 and MITF) in B16F10 cells; (E) schematic diagram showed the mechanisms of POS regulating melanogenesis through different signaling pathways. Results represented the means ± SEM of three independent experiments. $^{*}P < 0.05$, $^{**}P < 0.01$, $^{***}P < 0.001$, compared with non-treated group. AKT, protein kinase B; GSK, glycogen synthase kinase; MAPK, mitogen-activated protein kinase; MEK, mitogen-activated protein; ERK, extracellular signal-regulated kinases; JNK, c-Jun N-terminal kinase; TCA, tricarboxylic acid cycle; MITF, microphthalmia-associated transcription factor; TYR, tyrosinase; TRP, tyrosinase-related protein; SEM, standard error mean; POS, *Platycladus orientalis* shells.

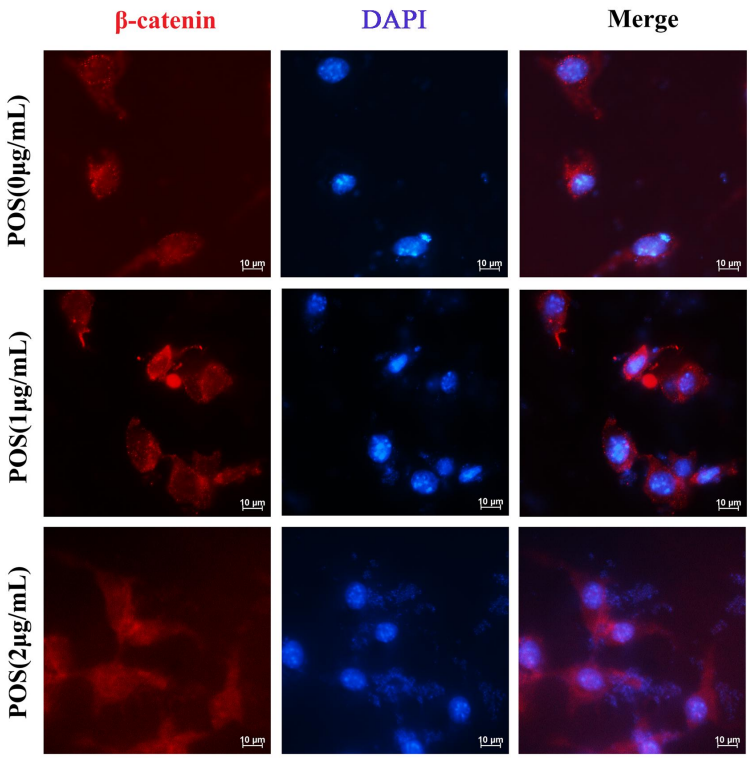

Figure 4 Immunofluorescence analysis of β-catenin protein in B16F10 cells. The result indicated that enrichment of β-catenin in the nucleus after POS treated. The β-catenin protein is shown in red, while the nucleus in blue. Data are representative of three independent experiments. DAPI, 4',6-diamidino-2-phenylindole; POS, *Platycladus orientalis* shells.

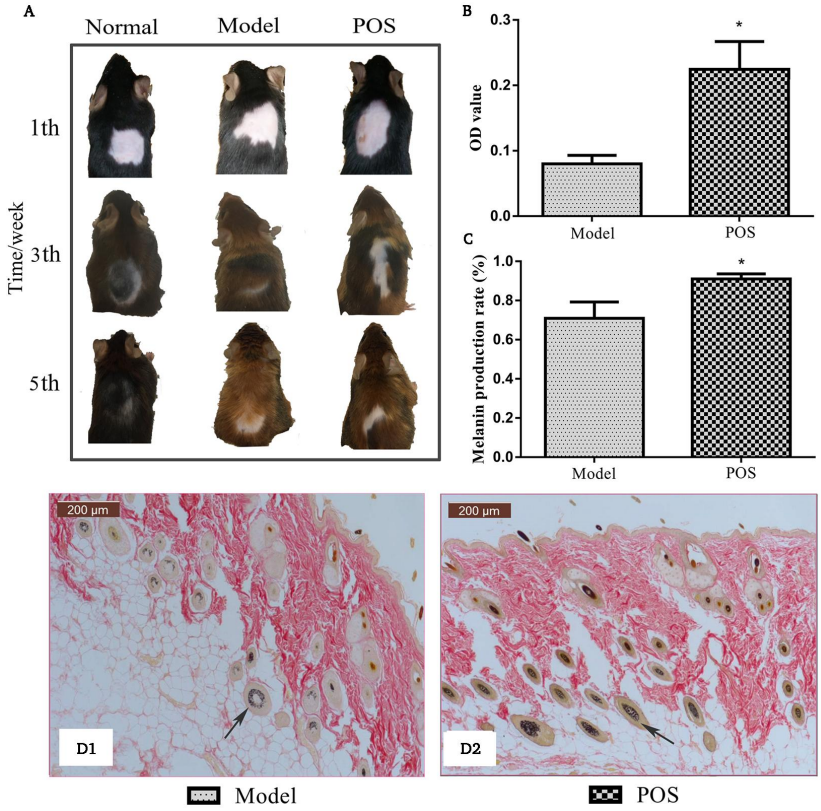

Figure 5 POS promotes melanogenesis and hair blacking in C57BL/6J mouse. (A) The depilation region photograph of C57BL/6J mouse; (B) the OD value of melanin in mice hair shaft; (C) melanin production rate in the shaved skin areas of mice (100×, n = 3); (D1) histology skin sections of mice in model group; (D2) histology skin sections of mice in POS group. Data are representative of three independent experiments. $^{*}P < 0.05$, compared with model group. OD, optical density; POS, *Platycladus orientalis* shells.

According to previous reports, the volatile oil components of POS mainly consisted of α-pinene (17.83%), Δ-3-carene (12.52%), β-caryophyllene (8.79%) and cedrol (12.44%) [21]. In our present research, the above components also appeared in POS. Cedrol occupied the largest percentage in POS (17.1%) (Table 2). As previous reported, cedrol as a fragrance ingredient in cosmetics and shampoos promoted hair growth, prevented hair follicle dystrophy and provided local protection against chemotherapy-induced alopecia [9]. In our experment, cedrol of equivalent concentrations (0.1 μg/mL and 0.2 μg/mL) display excellent effect of stimulated on melanogenesis (Figure 2E). Activation rate of the melanin content in B16F10 cells was 130 ± 7% at 0.2 μg/mL, which was slightly less than POS at 2 μg/mL (145 ± 8%). Therefore, cedrol exists in POS possibly played a crucial role in treatment of pigment disorder, other components in POS may also contribute to these effects

Subsequently, POS under safety concentration (1 μg/mL and 2 μg/mL) was treated to B16F10 cells. As a result, POS up-regulated the content of indole derivatives, increased melanin content and TYR activity. According to previous reports, melanogenesis depended on several steps including oxidization of L-tyrosine by TYR, catalysis and synthesis of indole derivatives by TRP-1 and TRP-2, and final formation of eumelanin [22]. As our experiment result, the content of 1H-indole-2-carboxylic acid and melanin was significantly increased in POS treated cells. Reverse transcription – polymerase chain reaction analysis indicated that mRNA levels of TYR, TRP-1,TRP-2 and MITF in B16F10 cells were enhanced by POS treatment. Meanwhile, POS increased the protein expression of TYR and MITF, enhanced enzyme activity of TYR. All these indicated that POS up-regulated melanin synthetic pathway. In addition, previous research showed that the increase of hexadecanoic acid and octadecanoic acid in melanoma was associated with their promotion of building block for plasmalogenes synthesis [23]. Fumaric acid was directly involved in the tricarboxylic acid cycle. Myo-inositol, as a derivative of Myo Inositol lipid, plays a significant role in lipid signaling and osmolarity regulation [24]. As shown in Table 3, POS increased the content of hexadecanoic acid, octadecanoic acid and fumaric acid compared with non-treated groups, which was likely to be a consequence of up-regulated de novo lipid synthesis in melanocytes. Additionally, POS obviously increased the level of myo-inositol compared with non-treated groups did which indicated that POS promote the synthesis and catabolism of fatty acids in melanocytes.

As previous report, MITF was regarded as an important regulative protein in melanogenesis [25]. MITF was involved in multiple signaling pathways, such as AKT, Wnt/β-catenin and MAPK signaling pathways [26, 27]. As shown in Figure 3 and Figure 4, POS significantly activated phosphorylation of p38 to increase the protein expression of MITF, inhibited phosphorylation of AKT to suppress MITF proteasomal degradation, increased phosphorylation of GSK3β to suppress β-catenin degradation, excessive β-catenin transferred to nucleus and thereby enhanced protein expression of MITF compared with non-treated groups [28–33] (Figure 3). These phenomenon indicated that POS promoted melanogenesis.

In conclusion, POS and cedrol displayed potential effect in treatment of pigmentation disorders and poliosis. POS increased TYR activity in potatoes and melanocytes and therefore up-regulated the content of indole derivatives and melanin in melanocytes. Cedrol was regarded as the main active substance for POS promoted melanogenesis. The possible mechanism involved in POS treatment of pigmentary disorders contained its promotion of lipid synthesis in melanocytes, activating p38 MAPK/MITF signaling pathway, inhibiting phosphorylation of AKT, increasing phosphorylation of GSK-3β, led to a decreased in the activity of GSK-3β and thereby suppressed β-catenin degradation. Then β-catenin begins to accumulated in the nucleus, and eventually activating MITF, TYR, TRP1 and TRP2. All in all, these phenomenon indicated that POS possessed potential for prevention against pigmentary disorders in B16F10 cells and C57BL/6J mice. These were merited further research for clinical application.

References

1. Gan DL, Yao Y, Su HW, et al. Volatile Oil of *Platycladus Orientalis* (L.) Franco leaves exerts strong anti-inflammatory effects via inhibiting the IkappaB/NF-kappaB pathway. *Curr Med Sci*. 2021;41(1):180–186. https://doi.org/10.1007/s11596-020-2301-2
2. Lin ZH, Liao WZ, Ren JY. Physicochemical characterization of a polysaccharide fraction from *Platycladus orientalis* (L.) Franco and its macrophage immunomodulatory and anti-Hepatitis B virus activities. *J Agric Food Chem*. 2016;64(29):5813–5823. https://doi.org/10.1021/acs.jafc.6b01387
3. Zhang Y, Han L, Chen SS, Guan J, Qu FZ, Zhao YQ. Hair growth promoting activity of cedrol isolated from the leaves of *Platycladus orientalis*. *Biomed Pharmacother*. 2016;83:641–647. https://doi.org/10.1016/j.biopha.2016.07.022
4. Shan MQ, Shang J, Ding AW. *Platycladus orientalis* leaves: a systemic review on botany, phytochemistry and pharmacology. *Am J Chin Med*. 2014;42(3):523–542. https://doi.org/10.1142/s0192415x14500347
5. Ren XY, Ye Y. Labdane diterpenes from the seeds of *Platycladus orientalis*. *J Asian Nat Prod Res*. 2006;8(8): 677–682. https://doi.org/10.1080/10286020500246584
6. Zhang NN, Park DK, Park HJ. Hair growth-promoting activity of hot water extract of *Thuja orientalis*. *BMC Complement Altern Med*. 2013;13:9. https://doi.org/10.1186/1472-6882-13-9
7. Zhang B, Zhang RW, Yin XQ, et al. Inhibitory activities of some traditional Chinese herbs against testosterone 5 alpha-reductase and effects of Cacumen platycladi on hair re-growth in testosterone-treated mice. *J Ethnopharmacol*. 2016;177:1–9. https://doi.org/10.1016/j.jep.2015.11.012
8. Deng, Y., et al. Hair growth promoting activity of *Cedrol nanoemulsion* in C57BL/6 mice and its bioavailability. *Molecules*. 2021;26(6):1795. https://doi.org/10.3390/molecules26061795
9. Chen SS, Zhang Y, Lu QL, Zhao YQ. Preventive effects of cedrol against alopecia in cyclophosphamide-treated mice. *Environ Toxicol Pharmacol*. 2016;46:270–276. https://doi.org/10.1016/j.etap.2016.07.020
10. Slominski RM, Sarna T, Płonka PM, Raman C, Brożyna AA, Slominski AT. Melanoma, melanin, and melanogenesis: the Yin and Yang relationship. *Front Oncol*. 2022;12:842496. https://doi.org/10.3389/fonc.2022.842496
11. Chaabane F, Pinon A, Simon A, Ghedira K, Chekir-Ghedira L. Phytochemical potential of Daphne gnidium in inhibiting growth of melanoma cells and enhancing melanogenesis of B16-F0 melanoma. *Cell Biochem Funct*. 2013;31(6):460–467. https://doi.org/10.1002/cbf.2919
12. Niu C. Aisa HA. Upregulation of melanogenesis and tyrosinase activity: potential agents for vitiligo. *Molecules*. 2017;22(8): 1303. https://doi.org/10.3390/molecules22081303
13. Jo, S.J., et al. The pattern of hair dyeing in koreans with gray hair. *Ann Dermatol*. 2013;25(4):401–404. https://doi.org/10.5021/ad.2013.25.4.401
14. Felsten LM, Alikhan A, Petronic-Rosic V. Petronic-Rosic. Vitiligo: a comprehensive overview Part II: treatment options and approach to treatment. *J Am Acad Dermatol*. 2011;65(3): 493–514. https://doi.org/10.1016/j.jaad.2010.10.043
15. Hu SH, Zhou G, Wang YW. Tyrosinase inhibitory activity of total triterpenes and poricoic acid A isolated from *Poria cocos*. *Chin Herb Med*. 2017;9(4):321–327. https://doi.org/10.1016/s1674-6384(17)60111-4
16. Lin YS, Wu WC, Lin SY, Hou WC. Glycine hydroxamate inhibits tyrosinase activity and melanin contents through downregulating cAMP/PKA signaling pathways. *Amino Acids*. 2015;47(3):617–625.

https://doi.org/10.1007/s00726-014-1895-8
17. Abrahamian C, Grimm C. Endolysosomal cation channels and MITF in melanocytes and melanoma. *Biomolecules*. 2021; 11(7):1021. https://doi.org/10.3390/biom11071021
18. Kim HJ, Kim JS, Woo JT, Lee IS, Cha BY. Hyperpigmentation mechanism of methyl 3,5-di-caffeoylquinate through activation of p38 and MITF induction of tyrosinase. *Acta Biochim Biophys Sin* (*Shanghai*). 2015;47(7):548–556. https://doi.org/10.1093/abbs/gmv040
19. Wu W, Yang J, Tao HJ, Lei MX. Environmental regulation of skin pigmentation and Hair Regeneration. *Stem Cells Dev*. 2022;31(5-6):91–96. https://doi.org/10.1089/scd.2022.29011.wwu
20. Xu GH, Ryoo IJ, Kim YH, Choo SJ, Yoo ID. Free radical scavenging and antielastase activities of flavonoids from the fruits of Thuja orientalis. *Arch Pharm Res*. 2009;32(2):275–282. https://doi.org/10.1007/s12272-009-1233-y
21. Rehman R, Hanif MA, Zahid M, Qadri RWK. Reporting effective extraction methodology and chemical characterization of bioactive components of under explored *Platycladus orientalis* (L.) Franco from semi-arid climate. *Nat Prod Res*. 2019;33(9): 1237–1242. https://doi.org/10.1080/14786419.2018.1519707
22. Zhou SH, Zeng HL, Huang JH, et al. Epigenetic regulation of melanogenesis. *Ageing Res Rev*. 2021;69:101349. https://doi.org/10.1016/j.arr.2021.101349
23. Abaffy T, Möller MG, Riemer DD, Milikowski C, DeFazio RA. Comparative analysis of volatile metabolomics signals from melanoma and benign skin: a pilot study. *Metabolomics*. 2013; 9(5):998–1008. https://doi.org/10.1007/s11306-013-0523-z
24. Milewska EM, Czyzyk A, Meczekalski B, Genazzani AD. Inositol and human reproduction. From cellular metabolism to clinical use. *Gynecol Endocrinol*. 2016;32(9):690–695. https://doi.org/10.1080/09513590.2016.1188282
25. Lee SM, Chen YS, Lin CC, Chen KH. Hair dyes resorcinol and lawsone reduce production of melanin in melanoma cells by tyrosinase activity inhibition and decreasing tyrosinase and microphthalmia-associated transcription factor (MITF) expression. *Int J Mol Sci*. 2015;16(1):1495–1508. https://doi.org/10.3390/ijms16011495
26. Lee N, Chung YC, Kim YB, Park SM, Kim BS, Hyun CG. 7,8-Dimethoxycoumarin stimulates melanogenesis via MAPKs mediated MITF upregulation. *Pharmazie*. 2020;75(2):107–111. https://doi.org/10.1691/ph.2020.9735
27. Levy C, Khaled M, Fisher DE. MITF: master regulator of melanocyte development and melanoma oncogene. *Trends Mol Med*. 2006;12(9):406–414. https://doi.org/10.1016/j.molmed.2006.07.008
28. Hartman ML, Czyz M. Pro-survival role of MITF in melanoma. *J Invest Dermatol*. 2015;135(2):352–358. https://doi.org/10.1038/jid.2014.319
29. Jung E, Kim JH, Kim MO, et al. Afzelin positively regulates melanogenesis through the p38 MAPK pathway. *Chem Biol Interact*. 2016;254:167–172. https://doi.org/10.1016/j.cbi.2016.06.010
30. Ko GA, Cho SK. Phytol suppresses melanogenesis through proteasomal degradation of MITF via the ROS-ERK signaling pathway. *Chem Biol Interact*. 2018;286:132–140. https://doi.org/10.1016/j.cbi.2018.02.033
31. Wang CY, Zhao L, Su Q, et al. Phosphorylation of MITF by AKT affects its downstream targets and causes TP53-dependent cell senescence. *Int J Biochem Cell Biol*. 2016;80:132–142. https://doi.org/10.1016/j.biocel.2016.09.029
32. Clevers H, Nusse R. Nusse. Wnt/beta-catenin signaling and disease. *Cell*. 2012;149(6):1192–1205. https://doi.org/10.1016/j.cell.2012.05.012
33. Hwang E, Lee TH, Lee WJ, et al. A novel synthetic Piper amide derivative NED-180 inhibits hyperpigmentation by activating the PI3K and ERK pathways and by regulating Ca^{2+} influx via TRPM1 channels. *Pigment Cell Melanoma Res*. 2016;29(1): 81–91. https://doi.org/10.1111/pcmr.12430